

A Deep Learning Approach to 3D Human Walking Pose Estimation From SensFloor Capacitive Signals

Anonymous Author(s)

Abstract

While camera-based systems are the dominant approach for human pose estimation, they face challenges in terms of privacy concerns and occlusion problems. These issues are of particular relevance in domains such as elderly care, where pose estimates can be used to monitor residents health or analyze incidents retrospectively. To assess an alternative to camera-based pose estimation, this paper aims to predict 3D walking poses using SensFloor: a capacitance-based floor which registers movement activity. We analyze the potential to utilize the floor's low-resolution signals to estimate poses and to what extent certain joint positions can be predicted accurately.

For this purpose, we collected synchronized SensFloor signals and video data, from which we extracted 3D human poses using MediaPipe to serve as ground-truth labels for training. These signals and their corresponding labels were then used for supervised training of an LSTM neural network. To estimate the person's position on the floor, a Kalman filter was applied to smooth the noisy SensFloor measurements.

Our results demonstrate that it is possible to predict human walking poses using the proposed methods, establishing a proof-of-concept for an alternative way of activity monitoring.

Keywords

SensFloor, Human pose estimation, Deep Learning, LSTM, Kalman Filter, Capacitive Floor, MediaPipe

Code: <https://github.com/sensfloor>

1 Introduction

With the ageing of the population elderly care is becoming more important than ever. However, the amount of missing workforces is increasing and is expected to be between 280 000 and 690000 in 2049 in Germany [1]. Therefore, the demand for AI-based technologies that support caregivers by automating monitoring tasks is growing, as they help improve patient safety even with limited personnel.

As monitoring patients for 24 hours continuously is particularly difficult with a limited workforce, research on estimating human movement and posture has been actively pursued.

In recent years, camera-based approaches for human pose estimation have been widely studied. However, such methods raise concerns regarding privacy and are sensitive to environmental factors such as occlusions and camera placement. Therefore, careful consideration is required before introducing these technologies in care facilities. To enable the practical implementation of automation in real care environments, it is necessary to explore alternative methods that can monitor patients while preserving privacy and mitigating occlusion issues.

Considering these concerns, one promising alternative for automating tasks in the real care-giving is floor-based sensing technology. In this study, we focus on SensFloor as an example of a

floor-based sensing system. SensFloor is primarily used in elderly care, as it provides a less intrusive form of monitoring compared to camera-based sensors. It is a capacitive sensing floor composed of rectangular patches, each containing eight triangular sensor fields. Each field registers changes in capacitance and outputs a signal between 127 and 255, depending on the magnitude of the detected change. Since the human body contains a large amount of water, walking over increases the change in capacitance, and SensFloor uses it to detect human movement.

Recently, various floor-based sensing approaches have been explored for human movement analysis. Several studies have estimated human posture or movement patterns using foot pressure-based sensors with neural network models, including intelligent carpets [1] and pressure-sensing insoles [2]. However, pressure-based systems capture richer information about foot–floor interactions than capacitive floor sensors. Moreover, existing studies using capacitive sensor floors [3] mainly focus on recognizing gait patterns or walking conditions, rather than estimating full-body 3D human poses. Therefore, while prior work demonstrates the potential of floor-based sensing for human movement analysis, the feasibility of estimating full-body 3D walking poses from low-resolution capacitive floor sensor signals remains largely unexplored.

In this study, we investigated the feasibility and accuracy of estimating human 3D walking poses from low-resolution SensFloor signals using a supervised neural network. we construct a supervised dataset by synchronizing SensFloor signals with video data, from which 3D human poses are extracted using MediaPipe and used as ground-truth labels. With this dataset, we train a supervised LSTM network to estimate 3D human poses solely from SensFloor signals. To evaluate the performance of our model, the predicted poses are compared with the ground-truth poses, and compute the error of sum of joints .

The results show that the accuracy of predicted poses achieved

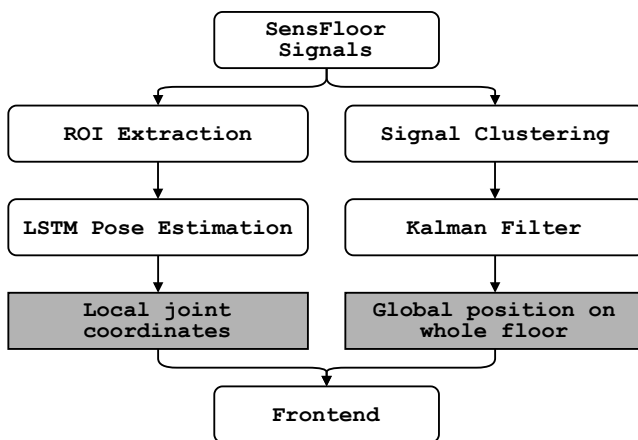
This study demonstrates the feasibility of estimating human poses using SensFloor without relying on cameras and provides the proof of concept for the practical human activity monitoring using SensFloor.

2 Methods

The final goal of this project is to design a system that reads SensFloor signals, processes them, and visualizes the person's gait within a virtual simulation. To achieve this goal, we split up the problem into two components: pose estimation and localization. The process of both components is illustrated in figure 1. By separating these tasks, the system is able to use a small localized active area of the floor for pose estimation. Afterward this pose is mapped across the global floor coordinates. This enables the system to be ported to various floors of different dimensions.

For the pose estimation component, we implemented a supervised fine-tuning pipeline. For that we collected reference pose

117 estimates from a MediaPipe to serve as labels. Using these labels,
 118 we trained a Long Short-Term Memory (LSTM) to predict human
 119 poses based on SensFloor activations within an extracted Region
 120 of Interest (ROI). To localize the estimated pose, a Kalman Filter
 121 processes the noisy sensor signals to determine the person's global
 122 coordinates. Finally, the combined data of pose and position is
 123 streamed to a frontend application for real-time visualization.
 124 [?]



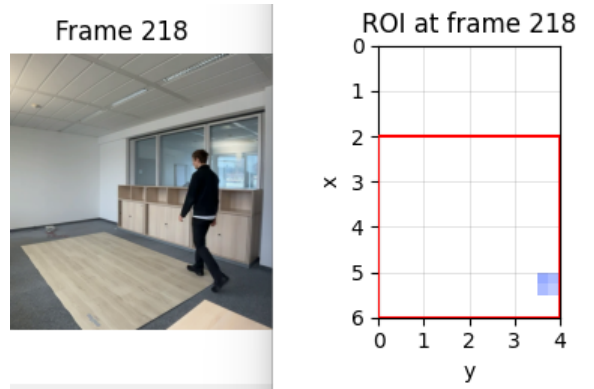
142 **Figure 1: Overview of the SensFloor-based pose estimation**
 143 **pipeline – The left branch estimates the pose in a local,**
 144 **position-independent coordinate system, while the right**
 145 **branch localizes the person in global floor coordinates.**

2.1 Data collection

The model developed in this paper takes SensFloor signals as input to predict the 3D joint coordinates of a person walking on the floor. To train and evaluate such a model, we recorded in two sessions a total of eight hours of synchronized SensFloor signals and video from three participants. To synchronize the data, we mapped the SensFloor signals to the corresponding video frame number at their time of occurrence. In post-processing, we used MediaPipe to extract 3D pose estimates from the video to serve as training targets. It is important to mention here that the origin of MediaPipe's pose estimates coordinate system is located at the center of the hips. This allows us to decompose the paper's problem into the previously mentioned two components of pose estimation relative to the hip and localization on the whole floor.

2.2 Training Data preprocessing

Before giving the data to our model we preprocess it in several ways. First we filter signals that are beneath a threshold and likely correspond to noise from the floor. We defined the threshold to be $\tau = 140$, but it can vary by the floor setup. Then we filter labels that do not contain SensFloor signals and vice versa ending up with a set of frames that contain both significant signals as input and a reference label. Next, we take the first 80% of this list as the training data, 10% as validation and 10% as test. When we load one item of this set we create a ROI history, which is a sequence of areas of the



175 **Figure 2: Example of one ROI in the sequence given to the**
 176 **model. The highlighted rectangle is the area of the ROI and**
 177 **the signals of the floor are in blue, showing the step of a**
 178 **person**

floor. We defined the sequence length as 50 and the ROI is a 4×4 grid of the floor with the signal values for this frame. The history is created by going back 50 frames and for each frame taking the signals it received or no signals if no signals were in this frame. All signals are normalized to the range $[0, 1]$ (127 will be 0 and 255 will be 1). Given the translation invariance of the data, we rotate the ROI history by 0, 90, 180, 270 randomly for a more robust training. Finally we use 13 of the 33 joints given by MediaPipe, excluding eyes, ears, mouth and fingers because they are irrelevant for our goal. Additionally we exclude the Foot heel and index, because MediaPipe predicted the foot unreliable to lengths of 3 cm to 18 cm.

2.3 Training Setup

We used a LSTM architecture for training our model. It is based on the model from [1]. We instead use a CNN to account for the Translation invariance. The full architecture is in figure 3. Instead of giving the model all signals of the floor, we construct a Region of Interest (ROI) which is a part of the floor containing the most signals in a defined sequence. A sequence is a collection of frames. For each frame we have a state of the floor. The state is constantly updated by the signals received from the patches. The CNN-LSTM model receives the signals in the ROI frame by frame and produces a vector with continuous values, the coordinate predictions for each joint. These coordinates are given into the Loss function. The total loss is defined as

$$L_{total} = L_{WMS} + \lambda \cdot L_{link}, \quad (1)$$

where λ is a fixed scalar for L_{link} . We set λ to 0.1. The L_{WMS} calculates the squared difference between predictions and the reference labels, the joint coordinates, weighted by specific landmark importance and is defined as

$$L_{WMS} = \frac{1}{B \cdot J \cdot 3} \sum_{i=1}^B \sum_{j=1}^J \sum_{k=1}^3 w_j (\hat{y}_{i,j,k} - y_{i,j,k})^2, \quad (2)$$

where B is the batch size, J the number of joints, k x,y and z coordinates of each joint, $\hat{y}_{i,j,k}$ the model's predictions and $y_{i,j,k}$

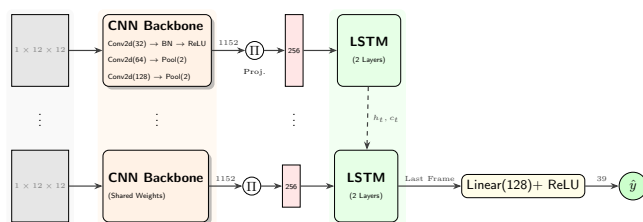
Patch signals should be explained
explain roi gird not tri-angular

212
213
214
215
216
217
218
219
220
221
222
223
224
225
226
227
228
229
230
231
232

233 the reference labels. We increased the weight for the knees and feet
 234 to 10 compared to 1 for everything else, because they are the most
 235 active components in a walking scenario Furthermore we used the
 236 link loss from [2] defined as
 237

$$L_{\text{link}}(d) = \begin{cases} k_{\min} - d, & \text{if } d < k_{\min} \\ d - k_{\max}, & \text{if } d > k_{\max} \\ 0, & \text{otherwise,} \end{cases} \quad (3)$$

242 where d is the length of a link (e.g. shoulder width) and k_{\min} and
 243 k_{\max} are the top and bottom 0.03 percentiles of the link lengths in
 244 the training set. We assume an upright position, this is why the
 245 upper body and the head will only rotate and the focus is more
 246 on the knee and feet MediaPipe extracts 33 Joints, we only used
 247 13, excluding the fingers, face expression, heels and foot index. For
 248 each epoch we calculate the following metrics: Mean joint position
 249 error (MJPE), percentage correct keypoints (PCK) with a 5 and 10
 250 threshold



260 **Figure 3: Overview of the model.** We used a CNN-LSTM ar-
 261 chitecture with a self attention layer
 262

264 We assume only one person is walking on the floor

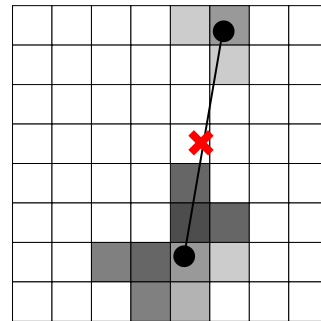
2.4 Localization

267 To integrate the local pose estimate from the model into the global
 268 coordinate system of the floor, we developed a pipeline that tracks
 269 the subject's hip position relative to the SensFloor. We do this by
 270 extracting a raw pose estimate through clustering the measured
 271 sensor activations and applying a Kalman filter to smoothen the
 272 trajectory.

273 We identify the subject's contact points with the floor by group-
 274 ing adjacent active sensor fields into clusters. The hip position
 275 is then calculated the following way: during a step, when both feet
 276 touch the ground, two clusters can be measured. In this case, we
 277 define the hip position as the midpoint between the centroids of the
 278 two clusters. If only one cluster is detected, meaning one foot is off
 279 the ground or both feet are close together, we assume the hip is lo-
 280 cated directly above that single centroid. This logic is illustrated in
 281 Figure 4 and allows us to extract the hip position from the received
 signals.

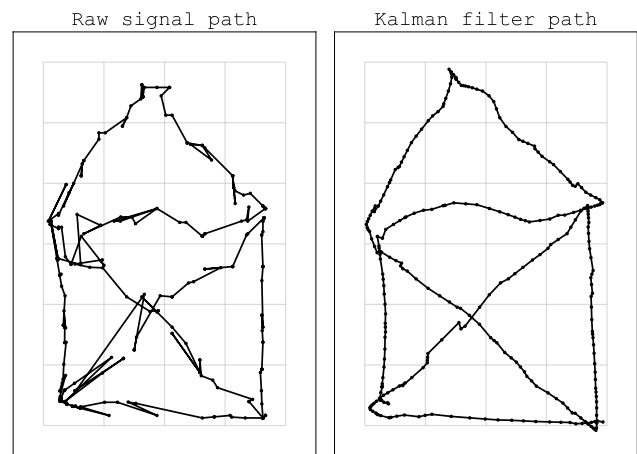
282 Because the raw position estimates are noisy and lead to jittery,
 283 unnatural movement in the visualization, we apply a Kalman Filter
 284 to ensure a smooth trajectory. Similar to [3, 255 ff], the filter's state
 285 vector is defined as $\mathbf{x} = [x, y, \dot{x}, \dot{y}]^T$, where x and y are the position
 286 coordinates and \dot{x} and \dot{y} the corresponding velocities. Due to the
 287 absence of ground-truth tracking data for exact calibration, we
 288 tuned the filter's noise parameters empirically until the trajectory

Is
this
dia-
gram
valu-
able
enough
for
the
space?



291
 292
 293
 294
 295
 296
 297
 298
 299
 300
 301
 302
 303
 304
 305
 306
 307
 308
 309
 310
 311
Figure 4: Calculation of the global position – This visualiza-
312
313
314
315
316
317
318
319
320
321
322
323
324
325
326
327
328
329
330
331
332
333
334
335
336
337
338
339
340
341
342
343
344
345
346
347
348
This visualization shows two clusters of SensFloor activations. For both the centroid calculated. The final position is then determined by taking the mean position between both clusters.

349 visually matched the subject's actual movement in the recorded
 350 videos. A comparison of the Kalman-filtered position estimates
 351 versus the raw positions is shown in Figure 5



352
 353
 354
 355
 356
 357
 358
 359
 360
 361
 362
 363
 364
 365
 366
 367
 368
 369
 370
 371
 372
 373
 374
 375
 376
 377
 378
 379
 380
 381
Figure 5: Effect of the Kalman filter – The left part of the im-
382
383
384
385
386
387
388
389
390
391
392
393
394
395
396
397
398
399
400
401
402
403
404
405
406
407
408
409
410
411
412
413
414
415
416
417
418
419
420
421
422
423
424
425
426
427
428
429
430
431
432
433
434
435
436
437
438
439
440
441
442
443
444
445
446
447
448
449
450
451
452
453
454
455
456
457
458
459
460
461
462
463
464
465
466
467
468
469
470
471
472
473
474
475
476
477
478
479
480
481
482
483
484
485
486
487
488
489
490
491
492
493
494
495
496
497
498
499
500
501
502
503
504
505
506
507
508
509
510
511
512
513
514
515
516
517
518
519
520
521
522
523
524
525
526
527
528
529
530
531
532
533
534
535
536
537
538
539
540
541
542
543
544
545
546
547
548
549
550
551
552
553
554
555
556
557
558
559
560
561
562
563
564
565
566
567
568
569
570
571
572
573
574
575
576
577
578
579
580
581
582
583
584
585
586
587
588
589
590
591
592
593
594
595
596
597
598
599
600
601
602
603
604
605
606
607
608
609
610
611
612
613
614
615
616
617
618
619
620
621
622
623
624
625
626
627
628
629
630
631
632
633
634
635
636
637
638
639
640
641
642
643
644
645
646
647
648
649
650
651
652
653
654
655
656
657
658
659
660
661
662
663
664
665
666
667
668
669
670
671
672
673
674
675
676
677
678
679
680
681
682
683
684
685
686
687
688
689
690
691
692
693
694
695
696
697
698
699
700
701
702
703
704
705
706
707
708
709
710
711
712
713
714
715
716
717
718
719
720
721
722
723
724
725
726
727
728
729
730
731
732
733
734
735
736
737
738
739
740
741
742
743
744
745
746
747
748
749
750
751
752
753
754
755
756
757
758
759
760
761
762
763
764
765
766
767
768
769
770
771
772
773
774
775
776
777
778
779
780
781
782
783
784
785
786
787
788
789
790
791
792
793
794
795
796
797
798
799
800
801
802
803
804
805
806
807
808
809
810
811
812
813
814
815
816
817
818
819
820
821
822
823
824
825
826
827
828
829
830
831
832
833
834
835
836
837
838
839
840
841
842
843
844
845
846
847
848
849
850
851
852
853
854
855
856
857
858
859
860
861
862
863
864
865
866
867
868
869
870
871
872
873
874
875
876
877
878
879
880
881
882
883
884
885
886
887
888
889
890
891
892
893
894
895
896
897
898
899
900
901
902
903
904
905
906
907
908
909
910
911
912
913
914
915
916
917
918
919
920
921
922
923
924
925
926
927
928
929
930
931
932
933
934
935
936
937
938
939
940
941
942
943
944
945
946
947
948
949
950
951
952
953
954
955
956
957
958
959
960
961
962
963
964
965
966
967
968
969
970
971
972
973
974
975
976
977
978
979
980
981
982
983
984
985
986
987
988
989
990
991
992
993
994
995
996
997
998
999
999

3 Results

4 Discussion and Conclusion

References

- [1] Raoul Hoffmann, Hanna Brodowski, Axel Steinlage, and Marcin Grzegorzek. 2021. Detecting Walking Challenges in Gait Patterns Using a Capacitive Sensor Floor and Recurrent Neural Networks. *21*, 4 (2021), 1086. doi:10.3390/s21041086
- [2] Yiyue Luo, Yunzhu Li, Michael Foshey, Wan Shou, Pratyusha Sharma, Tomas Palacios, Antonio Torralba, and Wojciech Matusik. 2021. Intelligent Carpet: Inferring 3D Human Pose from Tactile Signals. In *2021 IEEE/CVF Conference on Computer Vision and Pattern Recognition (CVPR)* (Nashville, TN, USA, 2021-06). IEEE, 11250–11260. doi:10.1109/CVPR46437.2021.01110
- [3] Roger R. and Labbe. 2024. Kalman and Bayesian Filters in Python. (2024). <https://github.com/rlabbe/Kalman-and-Bayesian-Filters-in-Python>